

## DETERMINATION OF LIMIT PORE SIZE DISTRIBUTIONS OF POROUS MATERIALS FROM MERCURY INTRUSION CURVES

M. C i e s z k o, M. K e m p i ń s k i

**Institute of Environmental Mechanics and Applied Computer Science  
Kazimierz Wielki University in Bydgoszcz  
Chodkiewicza 30, 85–064 Bydgoszcz, Poland**

The application of the capillary and chain models of pore architecture are proposed in the paper for determination of limit pore size distributions of porous materials based on the mercury intrusion curves. They estimate the range of pore sizes in the investigated material. It is proved that for a given pore size distribution, the capillary model of pore architecture, commonly used in the mercury porosimetry, and its chain model, are two limit cases of the network model of pore architecture, considered in the paper as a proper model for most real porous materials. For both limit pore architectures, the expressions describing capillary potential curves have been derived that are the basis for the procedure of determination of two limit pore size distributions. This procedure has been illustrated by determining the limit distributions for porous materials made of sintered glass beads.

### 1. INTRODUCTION

The distribution of pore diameters is the fundamental characteristics of the microscopic pore space structure of porous materials. It determines the basic macroscopic parameters of such materials (e.g. the volume porosity, permeability or the specific internal surface) that play an important role in many physical and chemical processes occurring in permeable porous materials, e.g. filtration, transport of mass, transport of the momentum and energy, wave propagation or chemical reactions [1, 2].

The common method of determination of pore diameters distribution is the interpretation of capillary potential curves obtained from the measurement of mercury intrusion into a porous sample [3–5] or from the measurement of the volume of a wetting fluid (water or ethyl alcohol) removed from the sample (e.g. by gas extrusion [6]) at progressively increasing pressure. Such an interpretation is most often based on the assumption that at increasing pressure, the mercury is intruded against the capillary forces into the pores of decreasing diameter. It is equivalent to the assumption that the pore structure of real porous material

can be modelled as a bundle of capillaries with random distribution of diameters. In that case the Washburn formula can be directly applied to interpretation of the experimental data. This formula relates fluid pressure with the diameter of cylindrical capillary in which the meniscus of a fluid is in the equilibrium state. As a result, the cumulative curves of volumetrical pore diameter distributions are obtained for porous material. The data obtained from fluid extrusion may be interpreted in the same way.

The capillary model does not account for situations that often occur in real porous materials, when the large pores are joined with one another by narrow necks making it impossible to fill with mercury at the pressure adequate to their diameter. This is an obvious shortcoming of this model because the volume pore size distribution determined by using it underestimate the volume of large pores in a sample, ascribing it to the volume of small pores. As a consequence, the obtained distributions are charged with a large error. The direct application of the Washburn formula in the interpretation of the capillary potential curves was also criticized in papers of other authors (e.g. [7, 8]).

Many attempts have been made to develop the network models of pore space that would improve the representation of the structure of real porous material (e.g. [9, 10] for 2D and [11–13] for 3D). They, however, have resulted in a very complicated description that often needs many computational efforts for carrying at a simulation of the mercury intrusion.

In the paper we propose to use the capillary and chain models of the pore architecture for determining the limit pore size distributions in porous materials on the basis of the capillary potential curves obtained by the mercury intrusion method. It has been proved that these models of pore architecture are the limit cases of its network model for a given pore size distribution. Therefore, the distributions determined by the capillary and chain models define the range of pore sizes in the investigated material. Such an approach is also justified by the fact that the accuracy of the mercury porosimetry is additionally limited by three other assumptions that are accounted for in the interpretation of the measured data, [8]: 1) the pores are cylindrical, 2) the wetting angle is constant, 3) the pore space remains undamaged during penetration.

The formulas describing the capillary potential curves of a layer of porous media with the capillary and chain pore architecture have been derived for a two-side intrusion of mercury. In these expressions the pore size distributions are present as a functional parameter. Proper selection of this function (e.g. by the optimization method) makes it possible to obtain the qualitative and quantitative compatibility of the theoretical and experimental capillary potential curves. This method was illustrated by determination of limit pore size distributions for the sample of porous material made of sintered glass beads.

## 2. MODELLING OF MERCURY INTRUSION INTO A LAYER OF POROUS MATERIAL

We consider models of pore space of porous materials in which the individual pores are cylindrical tubes (links) of equal length  $a$  and of random diameter  $D$  described by probability distribution  $\psi(D)$ . Two independent factors determine the pore space structure of such media: pore (link) diameter distribution  $\psi(D)$  and the way of their connection, the factor which we shall call the pore space architecture. Consequently, even for the same pore diameter distribution, the pore space structure may be different. Regarding the pore architecture we shall distinguish three kinds of models of the pore space structure: the capillary, chain and network models. In the capillary model the links of equal diameters are joined in a series to form long capillaries of constant diameters crossing the whole material. In the chain model the links are randomly joined in series to form capillaries of step-wise changing cross-section. In the network model, the randomly connected links form a spatial network.

In the paper we derive the capillary potential functions for a one-side and two-side intrusion of mercury into a layer of model porous media with the capillary and chain pore architecture. These functions are then applied in the proposed procedure for determination of the limit pore size distributions in porous materials based on the mercury intrusion curves.

### 2.1. The one-side intrusion model

To describe the static process of mercury intrusion into a layer of porous medium we first consider a system in which the porous material with initially empty pores occupies the halfspace  $z > 0$  and is in touch with mercury occupying the halfspace  $z < 0$ . We assume for the architecture of the skeleton pore space a chain model. This limits the complexity of the mathematical description of mercury intrusion into porous materials and simplifies the analysis of influence of the pore structure on the capillary potential curves.

Provided that mercury does not wet the surface of most materials, under pressure  $p$  the mercury will enter the capillaries of porous halfspace and its menisci will stop on those links for which the mercury pressure is balanced by the capillary pressure, i.e. on the links of diameter  $D$  that are smaller than diameter  $D^*$  defined by the Washburn expression

$$(2.1) \quad D^* = 4\sigma \cos \theta / p$$

where  $\sigma$  is the coefficient of mercury surface tension and  $\theta$  stands for the wettability angle of the skeleton material by mercury.

Links of diameters satisfying condition (2.1), following paper [14], will be called critical. They split all links into two classes. The first class is formed by the supercritical links of diameters larger than the critical one. These links may be filled with mercury at a given pressure. The other class is formed by subcritical links with diameters smaller than the critical one, filling of which with mercury at a given pressure is impossible. Using the proposed nomenclature, we can say that during the intrusion process, mercury fills only the first few supercritical links of capillaries until the first subcritical link occurs. Due to the statistical character of the link diameters and the constant value of its length, the depth of menisci placement in the capillaries will take random discrete values equal to the multiple length of the link. Only in the capillaries in which the first link is subcritical, the menisci occur on the surface of the porous halfspace.

Let a function  $F(z)$  denote the probability of mercury occurrence at the depth  $z$  of the porous halfspace. We can write

$$(2.2) \quad F(z) = \frac{m_z}{m_o}$$

where  $m_o$  is the mean number of capillaries in a unit area of the surface of porous halfspace and  $m_z$  stands for the number of capillaries in a unit area which are filled with mercury at the depth  $z$ . For  $z = 0$  we have

$$(2.3) \quad F(0) = 1,$$

and for  $0 < z \leq a$  function  $F(z)$  takes the form

$$(2.4) \quad F(z) = \eta$$

where

$$(2.5) \quad \eta = \int_{D^*}^{\infty} \psi(D) dD$$

define the probability of supercritical link occurrence among the first links of the capillaries. It is equal to the probability of supercritical link occurrence in the whole material.

Similarly to relation (2.2) we obtain expression for probability  $F(z - a)$  of mercury occurrence at the depth  $z - a$ ,

$$(2.6) \quad F(z - a) = \frac{m_{z-a}}{m_o}.$$

However, the probability of the event that capillaries filled at the depth  $z - a$  are also filled at the depth  $z$  is equal to the probability of supercritical link occurrence among the links joining levels  $z - a$  and  $z$ . We have

$$(2.7) \quad \frac{m_z}{m_{z-a}} = \eta.$$

Taking into account relations (2.2) and (2.6) we obtain the functional equation for probability  $F(z)$ ,

$$(2.8) \quad F(z) = \eta F(z - a).$$

Function  $F(z)$  has to fulfill conditions (2.3) and (2.4). Therefore, the solution of Eq. (2.8) takes the form

$$(2.9) \quad F(z) = \begin{cases} \eta^{[z/a]+1} & \text{for } z/a \notin \mathbb{N} \\ \eta^{[z/a]} & \text{for } z/a \in \mathbb{N} \end{cases}$$

where  $[z/a]$  denotes the integer part of the number  $z/a$ . It can be approximated by the upper limit function

$$(2.10) \quad F_U(z) = \eta^{z/a}$$

or by the lower limit function of the form

$$(2.11) \quad F_L(z) = \eta^{z/a+1}.$$

Function  $F(z)$  characterizes the mercury distribution in the porous halfspace during the intrusion process.

## 2.2. The two-side intrusion model

We apply function  $F(z)$  describing mercury distribution in the halfspace of porous media (2.9) (or its approximations (2.10) and (2.11)), to derive a mercury distribution function for the two-side mercury intrusion into a layer of thickness  $L$  (Fig. 1). In that case, the mercury intrusion may be considered as a two-step process: the left-hand side intrusion followed by the right-hand side one or vice versa. While the supercritical capillaries (composed of the supercritical links) are filled with mercury completely, the subcritical ones (containing also the subcritical links) remain partially empty. We shall consider the left- and right-hand side intrusions into the subcritical capillaries as separate processes, to determine determine function  $G(z)$  of mercury distribution in the layer that defines the probability of mercury occurrence at the depth  $z$  from the surface of the layer.

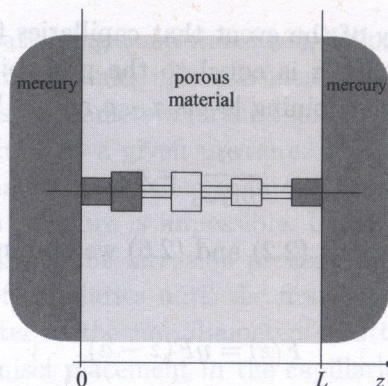


FIG. 1. The two-side intrusion of mercury into a layer of porous material with the chain architecture of the pore space.

Quantity

$$(2.12) \quad F(L) = \eta^N$$

defines the probability of mercury occurrence at the depth  $L = Na$  in a randomly chosen capillary (see (2.9)). Therefore, the number  $m_L$  of capillaries in a unit surface area of the layer, completely filled by mercury (the supercritical capillaries) during the left-hand side intrusion, is given by the formula

$$(2.13) \quad m_L = m_o F(L) = m_o \eta^N.$$

This means that the number  $m^S$  of capillaries partially filled with mercury (the subcritical capillaries) is equal to the difference of  $m_o$  and  $m_L$ . We obtain

$$(2.14) \quad m^S = m_o(1 - \eta^N).$$

Similarly, the number  $m_z^S$  of subcritical capillaries filled with mercury at the depth  $z$  during the left-hand side intrusion process is equal to the difference between the number  $m_z$  of all capillaries filled at the depth  $z$  in that process, given by expression (2.2), and the number  $m_L$  of supercritical capillaries. Therefore

$$(2.15) \quad m_z^S = m_o(F(z) - F(L)).$$

Since the left-hand side and right-hand side intrusions of mercury into subcritical capillaries of the layer are independent of each other, we can formulate a similar expression to (2.15) for the right-hand side intrusion of mercury. In that case the number  $m_s^S$  of subcritical capillaries filled with mercury at the depth  $s = L - z$ , taken from the right boundary surface of the layer, is given by expression

$$(2.16) \quad m_{L-z}^S = m_o(F(L - z) - F(L)).$$

The number  $m_z^T$  of all capillaries filled with mercury at the depth  $z$  induced by a two-side intrusion into the layer is equal to the sum of the number of supercritical capillaries and the number of all subcritical capillaries filled at this depth,

$$(2.17) \quad m_z^T = m_L + m_z^S + m_{L-z}^S .$$

Taking into account that the probability  $G(z)$  of mercury occurrence in the layer at the depth  $z$  can be defined as

$$(2.18) \quad G(z) = \frac{m_z^T}{m_o} ,$$

from relation (2.17) and (2.13), (2.15), (2.16) we have

$$(2.19) \quad G(z) = F(z) + F(L - z) - F(L) .$$

For the approximation defined by the lower limit function (2.11) we obtain

$$(2.20) \quad G(Z) = \eta(\eta^{NZ} + \eta^{N(1-Z)} - \eta^N)$$

where  $Z = z/L$ .

Mercury distributions in the layer of porous material for different values of pressures are shown in Fig. 2.

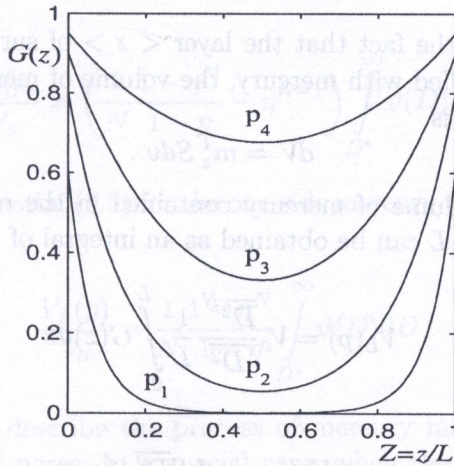


FIG. 2. Mercury distributions in the layer of porous material induced by a two-side intrusion at different pressures.

### 3. THE CAPILLARY POTENTIAL OF POROUS LAYER

We apply function  $G(z)$  of mercury distribution in the layer of porous medium to determine the relation between volume  $V_L(p)$  of the mercury intruded into

the layer of surface area  $S$  and mercury pressure  $p$ . Such relation is directly connected with the architecture of pores and their size distribution, and is called the capillary potential of porous material.

We denote by  $\langle z \rangle$  the infinitesimal layer of porous material of thickness  $dz$  placed in the porous layer at the depth  $z$ . Then, the mean volume  $dv$  of supercritical links in the layer  $\langle z \rangle$  is given by the expression

$$dv = \frac{\pi}{4} \overline{D^2}^N dz$$

where

$$(3.1) \quad \overline{D^2}^N = \frac{1}{\eta} \int_{D^*}^{\infty} D^2 \psi(D) dD$$

is the average value of the squared diameter of supercritical links.

Quantity  $\psi(D)/\eta$  can be interpreted as the probability distribution of link diameters in the set of supercritical links. It satisfies the condition

$$\int_{D^*}^{\infty} \psi(D)/\eta dD = 1.$$

Taking into account the fact that the layer  $\langle z \rangle$  of surface area  $S$  is crossed by  $m_z^T S$  capillaries filled with mercury, the volume of mercury  $dV$  contained in this part of the layer is

$$dV = m_z^T S dv.$$

Consequently, the volume of mercury contained in the porous layer of surface area  $S$  and thickness  $L$  can be obtained as an integral of the above relation,

$$(3.2) \quad V_L(p) = V_o \frac{\overline{D^2}^N}{\overline{D^2}} \frac{1}{L} \int_0^L G(z) dz$$

where

$$V_o = \pi m_o L S \overline{D^2} / 4$$

represents the total volume of pores in the distinguished part of the medium, whereas  $\overline{D^2}$  is the mean value of the squared diameter of all links.

From relation (3.2) we have

$$(3.3) \quad \frac{V_L(p)}{V_o} = \left( \frac{1}{\eta L} \int_0^L G(z) dz \right) \int_{D^*}^{\infty} \vartheta(D) dD$$

where

$$(3.4) \quad \vartheta(D) = D^2 \psi(D) / \overline{D^2}$$

can be interpreted as the volumetric probability distribution of the diameters of links. It characterizes the volume fraction of links of various diameters in the whole volume of pores. Therefore,

$$\int_0^\infty \vartheta(D) dD = 1.$$

Relation (3.3) describes the capillary potential curve of a layer of porous media for the two-side intrusion of mercury. For one-side intrusion it can be reduced to the form

$$(3.5) \quad \frac{V_L(p)}{V_o} = \left( \frac{1}{\eta L} \int_0^L F(z) dz \right) \int_{D^*}^\infty \vartheta(D) dD.$$

Using relation (2.20) for mercury distribution in the layer and expression (2.9), the function of capillary potential (3.3) for the two-side mercury intrusion takes the form

$$(3.6) \quad \frac{V_L(p)}{V_o} = \left( \frac{2}{N} \frac{1 - \eta^N}{1 - \eta} - \eta^{N-1} \right) \int_{D^*}^\infty \vartheta(D) dD,$$

and the capillary potential (3.5) for the one-side mercury intrusion can be rewritten as

$$(3.7) \quad \frac{V_L(p)}{V_o} = \frac{1}{N} \frac{1 - \eta^N}{1 - \eta} \int_{D^*}^\infty \vartheta(D) dD.$$

The above relations describe the process of mercury intrusion into a layer of chain architecture of pores. In a special case, when the length of the links in chains is equal to the thickness of the layer, the chain architecture of pores in a layer reduces to the capillary architecture. Then  $N = 1$ , and from (3.6) and (3.7) we obtain

$$(3.8) \quad \frac{V_L(p)}{V_o} = \int_{D^*}^\infty \vartheta(D) dD.$$

#### 4. INFLUENCE OF PORE ARCHITECTURES ON THE CAPILLARY POTENTIAL OF POROUS MATERIAL

Above we have obtained three different functions for the capillary potential of a porous layer. For the chain model at one-side and two-side mercury intrusion, these functions are given by formulas (3.7) and (3.6), respectively, and for the capillary model by formula (3.8). From their form it results that the volume fraction of pores filled with mercury at a given pressure is defined by the product of two quantities: the volume fraction of supercritical links in the layer,

$$\int_{D^*}^{\infty} \vartheta(D) dD ,$$

and the coefficient characterizing the degree of filling of the supercritical links with mercury. This coefficient depends on the pore architecture of porous medium, on the way of mercury intrusion and number  $N = L/a$  of links in each capillary. Its form determines the difference between functions (3.6)–(3.8) of the capillary potential. These functions indicate that only in the capillary model all supercritical links are filled. It is an obvious disadvantage of this model.

The capillary potential curves for the two-side mercury intrusion into a porous layer with the capillary and chain architecture of the pore space structure are shown in Fig. 3 (solid curves). It was assumed that the pore diameter distribution in both cases are described by three parametric rational function of the form

$$(4.1) \quad \psi(D) = \frac{m+n}{2\pi D_0} \sin\left(\frac{n-1}{m+n}\pi\right) \frac{(D/D_0)^m}{1+(D/D_0)^{m+n}} .$$

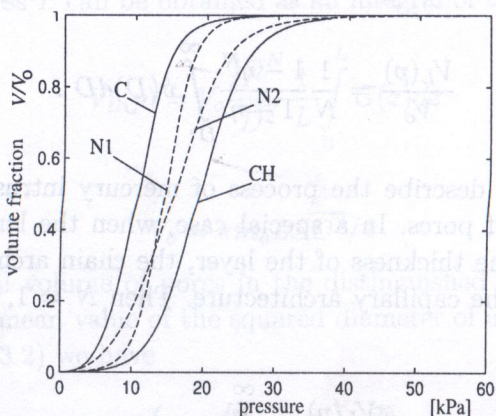


FIG. 3. Capillary potential curves of porous layer for capillary (C), chain (CH) and network (N1, N2) pore architectures and the same pore diameter distribution.

This ensures that pore distributions in the ranges of small and large pore diameters are power functions. Parameter  $m$  is the power of limit distribution in the range of small pore diameters ( $D \ll D_o$ ), whereas  $n$  is the power in the range of their large values ( $D \gg D_o$ ). Parameters  $m$ ,  $n$  and  $D_o$  of the distribution function  $\psi(D)$  are related to the average values of pore diameter  $\bar{D}$  and their square  $\bar{D}^2$  by

$$(4.2) \quad \bar{D} = D_o \frac{\sin(\pi(n-1)/(m+n))}{\sin(\pi(n-2)/(m+n))}, \quad \bar{D}^2 = D_o^2 \frac{\sin(\pi(n-1)/(m+n))}{\sin(\pi(n-3)/(m+n))}.$$

Both graphs in Fig. 3 have been drawn up for the same values of parameters of function  $\psi(D)$ :  $m = 3$ ,  $n = 6$ ,  $D_o = 0.1$  mm at  $N = 30$ ,  $\sigma = 0.485$  N/m and  $\theta = 130^\circ$ . It means that in both cases the pore volume distributions in the layer are identical. Therefore, the difference between the capillary potential curves in Fig. 3 characterizes the degree of their dependence on the pore architecture in the layer. From Fig. 3 it results that in the whole range of pressures the volume of mercury intruded into the porous layer with the chain pore architecture is smaller than the volume of mercury intruded at the same pressure into the layer with the capillary pore architecture. At the same time both curves are the limit capillary potential curves which, for a given length and diameter distribution of links, can have porous media of any net architecture.

In the capillary model all supercritical links of the porous layer are filled with mercury at a given pressure, whereas in the chain model the number of supercritical links filled with mercury is minimal due to the lack of connections between the chains of the links. The occurrence of such connections in a porous medium changes the chain pore architecture into the network type, and results in an increased number of supercritical links filled with mercury at a given pressure. This is possible because of a greater number of ways through which the links can be filled. Consequently, the capillary potential curves for porous material of the network architecture have to lie between the capillary potential curves for the media of the capillary and chain pore architectures and the same pore diameter distribution. In that sense the capillary and chain models are two limit cases of the network models. Therefore, the functions of the capillary potential for both limit cases can be considered as the estimating functions for the capillary potential of network models.

The two dashed curves in Fig. 3 are drawn to represent the exemplary potential curves of a porous material with two different network architectures of pore space, the links of which are of the same length and pore diameter distribution as the links of the capillary and chain models. It can be seen in Fig. 3, that capillary potential curves of porous materials depend both on the pore diameter distribution and on the pore architecture of their pore space.

## 5. ESTIMATION OF PORE SIZE DISTRIBUTION

The procedure used for determination of the pore size distribution of porous materials in the mercury porosimetry must be based on a theoretical model describing the process of mercury intrusion into a porous sample. Its accuracy depends on the degree of compatibility between the assumed model of pore space structure and the structure of the investigated material. Due to the complexity of pore structure of real porous materials, such models are still subject to study. Therefore, in the standard mercury porosimetry the pore size distributions are determined using a simple, capillary model of pore space structure.

In this section we will show that the application of capillary and chain models of pore architecture for interpretation of the mercury intrusion curves makes it possible to determine the limit pore diameter distributions defining the incidence of real diameter distribution in the investigated material. In our considerations we assume that the network model is a good representation of the pore space architecture of permeable porous materials and we use the fact that the capillary and chain models are limit cases of the network model. In this case the capillary potential curve of a sample of porous material obtained from the mercury porosimeter can be interpreted as a curve determined for porous sample of the network architecture of pore space. Therefore, according to the analysis of the previous section, the measured curve will be contained between the potential curves for materials of the capillary and chain architectures of pores and the same pore diameter distribution (Fig. 3). The pore size distribution could be determined from each of those three capillary potential curves provided that we use for their interpretation a proper model of mercury intrusion. However, in the case of a network model, although we know the experimental potential curve, we don't know its theoretical description. In the two other models the situation is the opposite. The theoretical descriptions are known whereas the experimental curves of capillary potential are not known. It means that the exact determination of the pore diameter distribution is impossible.

Therefore, we shall use capillary and chain models for interpreting the capillary potential curves obtained from the mercury porosimeter. Such a procedure is interesting because it enables us to determine two different distributions that limit the range of pore diameter distribution in the porous material. It follows from the fact that independently of the model of pore architecture, the displacement of the capillary potential curve towards greater pressures (Fig. 3) corresponds to the displacement of the pore diameter distribution towards smaller diameters, and inversely. Therefore, interpretation of the capillary potential curve of porous sample by means of the capillary model enables us to determine the lower limit distribution of pore diameters, whereas such interpretation by means

of the chain model allows us to determine the upper limit distribution. It is a direct consequence of the fact that the capillary potential curves for the network model of pore architecture lie between such curves for capillary and chain models.

The pore diameter distributions corresponding to the capillary potential curves presented in Fig. 3 are shown in Fig. 4. The solid curve (R) represents the diameter distribution of links used in the previous section to draw the graphs of capillary potentials for porous samples of capillary and chain pore architectures (solid lines in Fig. 3). This curve also represents the link diameter distribution in porous sample of network architecture, the capillary potentials of which are shown in Fig. 3 by dashed lines N1 and N2. The dashed lines in Fig. 4 were used to show the limit curves of pore diameter distributions. They were determined from the capillary potential curves N1 and N2 using expressions (3.6) and (3.8) for the chain and capillary models of pore architecture and the standard optimization procedure. Lines  $N1_C$  ( $m = 5.06$ ,  $n = 8.11$ ,  $\bar{D}_o = 0.08$  mm) and  $N1_{CH}$  ( $m = 4.19$ ,  $n = 5.95$ ,  $\bar{D}_o = 0.12$  mm) in Fig. 4a represent limit distributions for curve N1, whereas lines  $N2_C$  ( $m = 3.20$ ,  $n = 5.51$ ,  $\bar{D}_o = 0.06$  mm) and  $N2_{CH}$  ( $m = 2.14$ ,  $n = 4.32$ ,  $\bar{D}_o = 0.14$  mm) in Fig. 4b represent such distributions for curve N2. The average diameters of links calculated from these distributions are:

$$\begin{aligned} \bar{D}_{1C} &= 0.08 \text{ mm}, & \bar{D}_{1CH} &= 0.126 \text{ mm}, \\ \bar{D}_{2C} &= 0.066 \text{ mm}, & \bar{D}_{2CH} &= 0.154 \text{ mm}. \end{aligned}$$

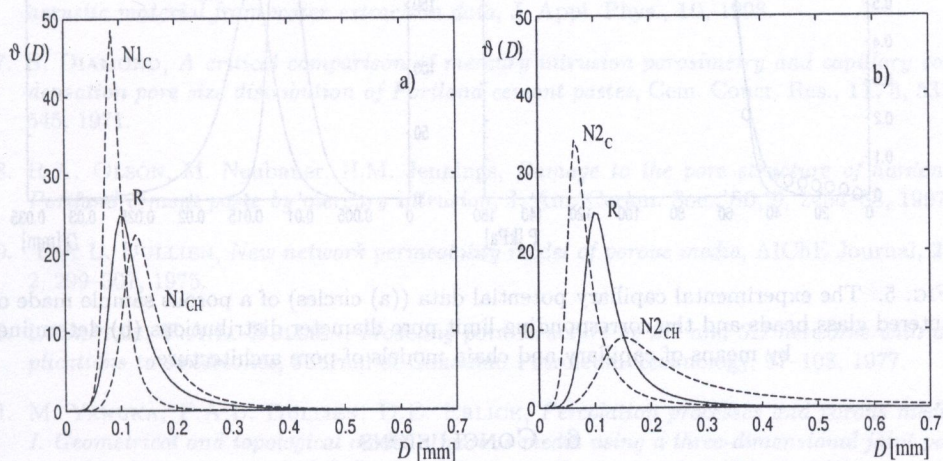


FIG. 4. The volumetrical distribution of pore diameters in a porous material (solid lines) and their limit distributions (dashed lines) determined from capillary potential curves N1 (a) and N2 (b) shown in Fig. 3.

Diameters  $\bar{D}_{1C}$  and  $\bar{D}_{1CH}$  estimate the real mean value  $\bar{D}_R = 0.1$  mm of pore diameters in a porous sample of network pore architecture for which the capillary potential is given by the curve N1 (see Fig. 3), whereas numbers  $\bar{D}_{2C}$  and  $\bar{D}_{2CH}$  estimate the value  $\bar{D}_R$  in a sample of capillary potential given by the curve N2.

The developed procedure has been illustrated by determination of the limit pore diameter distributions for a porous material made of sintered glass beads of mean diameter 80  $\mu\text{m}$ . Points of the capillary potential data determined by means of the porosimeter Autopore 9220 are presented in Fig. 5a (circles). Both limit pore diameter distributions are shown in Fig. 5b. Curves  $N_C$  ( $m = 3.748$ ,  $n = 20.951$ ,  $\bar{D}_o = 0.0122$  mm) and  $N_{CH}$  ( $m = 6.012$ ,  $n = 9.423$ ,  $\bar{D}_o = 0.0143$  mm) represent distributions obtained from the capillary potential data of sintered porous material using the capillary (see (3.8)) and chain (see (3.6)) models of pore architecture, respectively, and the standard optimization procedure. Solid lines in Fig. 5a are the capillary potential curves obtained from (3.8) and (3.6) for parameters of diameter distributions determined in the optimization procedure. They illustrate the accuracy of description of the experimental capillary potential curve by theoretical functions obtained for both models.

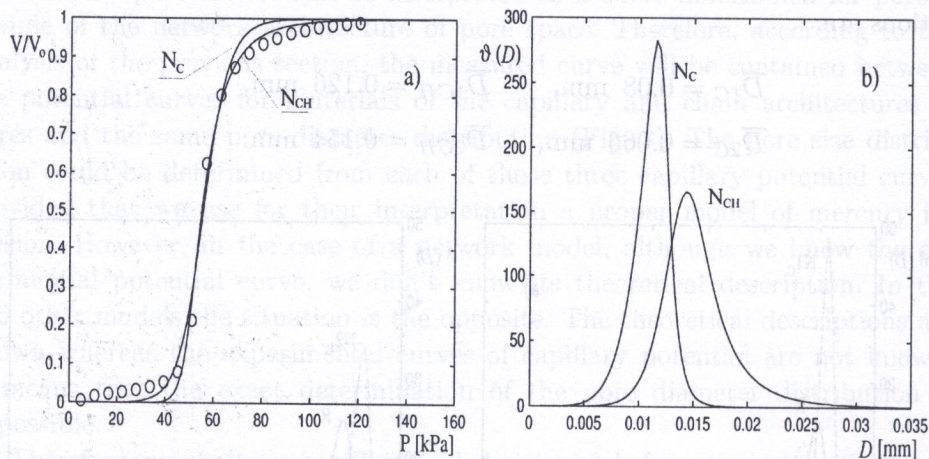


FIG. 5. The experimental capillary potential data ((a) circles) of a porous sample made of sintered glass beads and the corresponding limit pore diameter distributions (b) determined by means of capillary and chain models of pore architecture.

## 6. CONCLUSIONS

It has been shown that the capillary model of pore space architecture, commonly used for interpretation of experimental data of the mercury porosimetry and its chain model, are two limit cases of the network models provided that they

have the same pore size distribution. It has been proved that capillary potential curve for a medium with network pore architecture is always placed between such curves for the media with capillary and chain pore architecture. For both the limit models, simple expressions for the capillary potential have been derived. They describe the capillary potential curves for a layer of porous material for two-side mercury intrusion. They are proposed to be used for determining the limit pore size distributions defining the range of pore sizes in the investigated material. The capillary model enables determination of the lower limit distribution of pore diameters, whereas the chain model determines their upper limit distribution.

## REFERENCES

1. A.E. SCHEIDEGER, *The physics of flow through porous media*, Univ. Press, Toronto 1957.
2. F.A.L. DULLIEN, *Porous media*, Academic Press, New York 1979.
3. C.A. LEÓN Y LEÓN, M.A. THOMAS, *Recent advances in the interpretation of mercury porosimetry data*, GIT Laboratory Journal, **1**, 101–104 1997.
4. D.N. WINSLOW, *Advances in experimental techniques for mercury intrusion porosimetry*, Surf. Colloid Sci., **13**, 259–82 1984.
5. P.A. WEBB, C. ORR, *Analytical methods in fine particle technology*, Micrometetics Instrument Corporation, Norcross, GA USA, 1997.
6. P. LECLAIRE, M.J. SWIFT, V. HOROSHENKOV, *Determining the specific area of porous acoustic material from water extraction data*, J. Appl. Phys., **10**, 1998.
7. S. DIAMOND, *A critical comparison of mercury intrusion porosimetry and capillary condensation pore size distribution of Portland cement pastes*, Cem. Concr. Res., **11**, 5, 531–545, 1971.
8. R.A. OLSON, M. Neubauer, H.M. Jennings, *Damage to the pore structure of hardened Portland cement paste by mercury intrusion*, J. Am. Ceram. Soc., **80**, 9, 2454–58, 1997.
9. F.A.L. DULLIEN, *New network permeability model of porous media*, AIChE Journal, **21**, 2, 299–307, 1975.
10. I. CHATZIS, F.A.L. DULLIEN, *Modeling pore structure by 2D and 3D networks with applications to sandstones*, Journal of Canadian Petroleum Technology, 97–108, 1977.
11. M. YANUKA, F.A.L. DULLIEN, D.E. ERLICK, *Percolation processes and porous media, I. Geometrical and topological model of porous media using a three-dimensional joint pore size distribution*, Journal of Colloid and Interface Science, **112**, 1, 24–41 1986.
12. G.P. MATTHEWS, A.K. MOSS, M.C. SPEARING, F. VOLAND, *Network calculation of mercury intrusion and absolute permeability in sandstone and other porous media*, Powder Technology, **76**, 95–107 1993.

- 13. J.E.P. MONTEAGUDO, K. RAJAGOPOL, P.L.C. LAGE, *Scaling laws in network models: porous medium property prediction during morphological evolution*, Journal of Petroleum Science and Engineering, **32**, 179-190 2001.
- 14. I.A. CHUZMADZHEW, W.S. MARKIN, M.R. TRANSEWICH, *Macrokinetics of processes in porous media* [in Russian], Nauka, Moscow 1971.

Received June 15, 2005; revised version March 10, 2006.

REFERENCES

1. D.N. WINSLOW, Advances in experimental techniques for porous medium permeability, *Int. J. Colloid Interface Sci.*, **13**, 280-321 1964.

2. P. A. WARD, C. ORR, Analytical methods in fine particle technology, *Chromatography Instrument Corporation*, Newark, CA USA, 1997.

3. P. LECIAIRE, M. J. SWIRT, V. HOROSHERKOV, Determining the specific area of porous ceramic material from water extraction data, *J. Appl. Phys.*, **10**, 1998.

4. S. DIAMOND, A critical comparison of mercury intrusion porosimetry and capillary condensation pore size distribution of Portland cement pastes, *Can. Concr. Res.*, **11**, 5, 531-545, 1971.

5. R. A. OLSON, M. NEUBAUER, H.M. JENNINGS, Damage to the pore structure of hardened Portland cement paste by mercury intrusion, *J. Am. Ceram. Soc.*, **80**, 2, 257-28, 1997.

6. T. A. L. DULLER, New network permeability model of porous media, *AIChE Journal*, **31**, 2, 399-397, 1975.

7. T. A. L. DULLER, Permeability prediction for porous media using 2D and 3D networks, *Int. J. Numer. Anal. Methods in Fluids*, **10**, 1, 1-10, 1977.

8. M. YANUKA, F. A. J. DULLER, D. E. BRICK, Prediction processes and porous media. A geometrical and topological model of porous media using a three-dimensional joint pore size distribution, *Journal of Colloid and Interface Science*, **112**, 1, 34-41 1985.

9. G. MATHIAS, A. K. MOSE, M. C. SPERANDI, F. VOLARD, Network calculation of permeability and tortuosity in porous media, *Journal of Applied Physics*, **67**, 1, 1-10, 1990.